# Origin of photoinduced metastable defects in amorphous chalcogenides

K. Shimakawa, S. Inami, and T. Kato
*Department of Electronics and Computer Engineering, Gifu University, Gifu 501-11, Japan*

S. R. Elliott
*Department of Chemistry, University of Cambridge, Lensfield Road, Cambridge, England*
(Received 23 March 1992; revised manuscript received 14 July 1992)

Prolonged exposure to band-gap light decreases the photoconductivity of annealed films of amorphous chalcogenides ($As_2S_3$, $As_3S_7$, AsS, $As_2Se_3$, $GeS_2$, $GeSe_2$, and GeSe). This can be attributed to photoinduced metastable defects, which could act as additional trapping and/or recombination centers. These metastable centers are removed by annealing near the glass transition temperature. The kinetics of the temporal change of photocurrent during illumination are discussed in a model of defect-conserved bond switching.

## I. INTRODUCTION

Photoinduced defect creation in amorphous chalcogenides has been studied using light-induced electron-spin resonance (LESR),[1,2] xerographic,[3,4] ac transport,[5,6] and photocurrent[7,8] measurements. A model has been presented in our earlier studies[7,8] for the light-induced creation of metastable deep defect states in stoichiometric amorphous chalcogenides [e.g., $As_2S(Se)_3$, $GeS(Se)_2$]. The reversible time-dependent changes in the photoconductivity caused by optical illumination result from the initial creation of intimate pairs (IP) of charged defects (previously referred to as self-trapped excitons[5-8]), followed by bond-switching reactions leading to widely separated, metastable "random pairs" (RP) of defects.

In the present paper, through measurements of the temperature-dependent decrease in photocurrent $I_p$ for stoichiometric amorphous $As_2S_3$, $As_2Se_3$, $GeS_2$, and $GeSe_2$ films, and off-stoichiometric amorphous $As_3S_7$, AsS, and GeSe films, the kinetics of defect-conserved bond-switching (DCBS) reactions are discussed using a potential-energy diagram for IP and RP centers. The kinetics of DCBS may be "dispersive"[9,10] in nature and hence the temporal change in $I_p$ can be expressed empirically by using the stretched exponential term $[\exp(Ct^{\alpha})]$, where $0<\alpha<1$. Fitting to the experimental data produces information about the magnitude of the potential barriers associated with the formation of IP and RP centers.

## II. PHOTOCONDUCTIVITY STUDIES

Thin films of amorphous $As_2S_3$, $As_3S_7$, AsS, $As_2Se_3$, $GeS_2$, $GeSe_2$, and GeSe were evaporated onto Corning 7059 substrates. After evaporation, the samples were annealed at appropriate temperatures below the glass-transition temperature $T_g$. The thickness of the films, the annealing temperatures $T_a$, and the Tauc gap $E_0$ are given in Table I. The actual compositions of As-S(Se) films were estimated using x-ray photoemission spectroscopy (XPS) measurements and these are shown in parentheses in Table I. Sulfur-rich films compared with the starting glasses were always obtained. Planar gap cell electrodes using Al contacts were fabricated (gap spacing 40 $\mu$m, gap width 5 mm). The applied voltages were 300 V for S-containing materials and 5 V for Se-containing materials. A halogen lamp (57 mW/cm$^2$), or a high-pressure mercury lamp (54 mW/cm$^2$) for wider band-gap materials, was used with an ir-cut water filter to induce photoconductivity. The type of lamp used in each case is

TABLE I. Experimental details. Film thickness, annealing temperature $T_a$ after evaporation and photoillumination, glass-transition temperature $T_g$, Tauc gap $E_0$, and excitation lamp used for illumination (M, mercury; H, halogen).

| Chalcogenide | Thickness ($\mu$m) | Annealing temperature $T_a$ (°C) | Glass-transition temperature $T_g$ (°C) | Tauc gap $E_0$ (eV) | Lamp |
|---|---|---|---|---|---|
| $As_2S_3$ ($As_{1.9}S_{3.1}$) | 1.0 | 170 (2 h) | 200 | 2.44 | M |
| $As_3S_7$ ($As_{2.9}S_{7.1}$) | 0.7 | 125 (2 h) | 150 | 2.57 | M |
| AsS ($AsS_{1.1}$) | 0.4 | 115 (2 h) | 140 | 2.28 | M |
| $As_2Se_3$ ($As_{2.0}Se_{3.0}$) | 0.9 | 160 (2 h) | 190 | 1.79 | H |
| $GeS_2$ | 1.2 | 300 (1 h) | 480 | 2.64 | M |
| $GeSe_2$ | 1.5 | 250 (1 h) | 420 | 2.04 | H |
| GeSe | 1.0 | 200 (1 h) | | 1.40 | H |

 

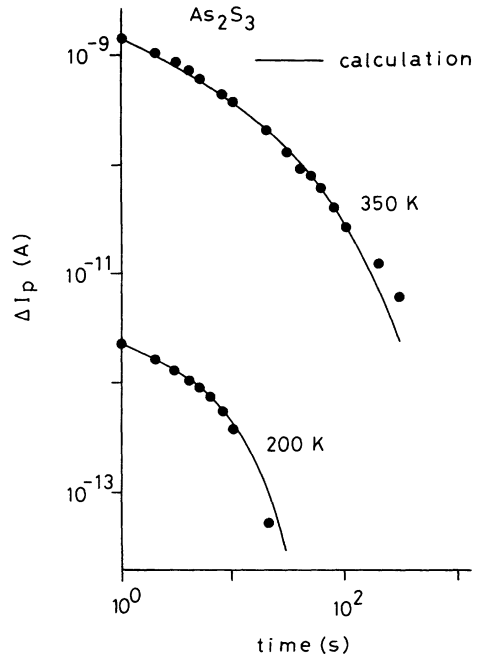


FIG. 1. Time-dependent change in photocurrent, $\Delta I_p$ for *a*-$As_2S_3$ measured at 200 and 350 K, where $\Delta I_p$ is defined as $I_p - I_\infty$. The solid lines are fits to Eq. (4).

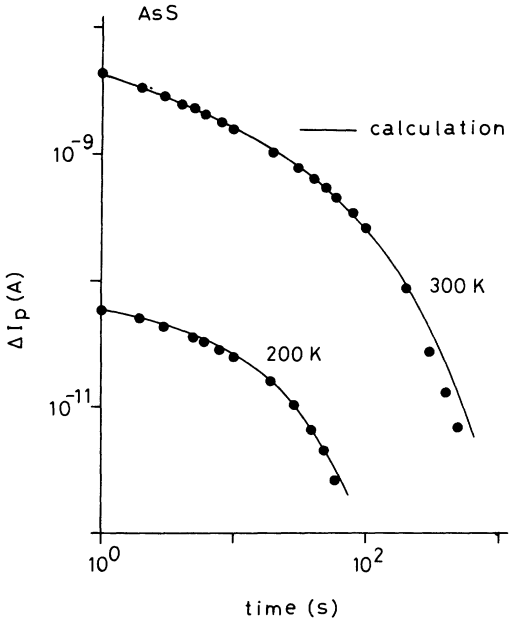


FIG. 3. Time-dependent change in photocurrent, $\Delta I_p$ for *a*-AsS at 200 and 300 K. The solid lines are fits to Eq. (4).

also given in Table I. A more detailed description of the experimental procedures is given in an earlier paper.[7]

During illumination, the photocurrent $I_p$ decreases with time and approaches a constant value $I_\infty$. The solid circles in Figs. 1–3 show examples of the time-dependent change in photocurrent measured at different temperatures for stoichiometric $A_2S_3$, S-rich $As_3S_7$, and As-rich AsS films, respectively, where $\Delta I_p(t)$ is defined as $I_p(t) - I_\infty$. Restoring $I_p$ to the original well-annealed state requires annealing to $T_a$ (see Table I), irrespective of whether illumination was carried out at low or high temperatures. The solid lines in Figs. 1–3 represent the cal-

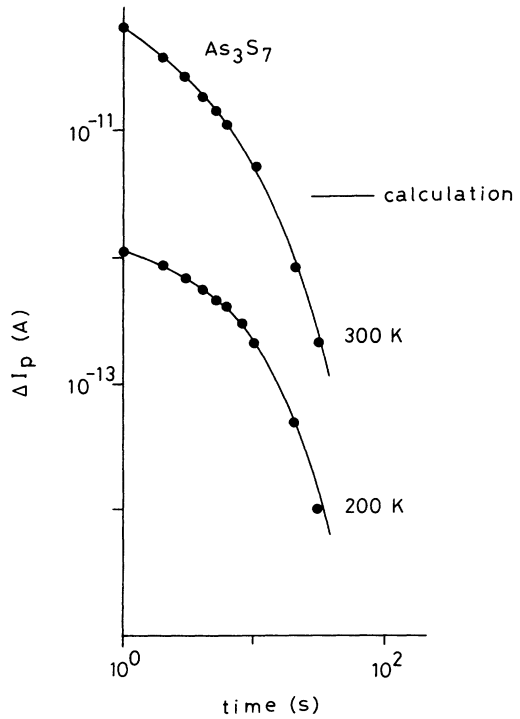


FIG. 2. Time-dependent change in photocurrent, $\Delta I_p$ for *a*-$As_3S_7$ at 200 and 300 K. The solid lines are fits to Eq. (4).

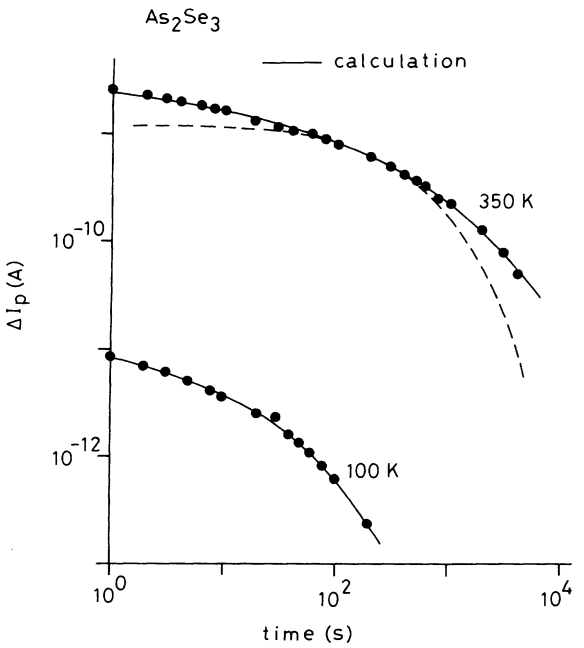


FIG. 4. Time-dependent change in photocurrent, $\Delta I_p$ for *a*-$As_2Se_3$ at 100 and 350 K. The solid lines are fits to Eq. (4) and the dashed line is fit to $\alpha = 1$ (exponential) in Eq. (4).

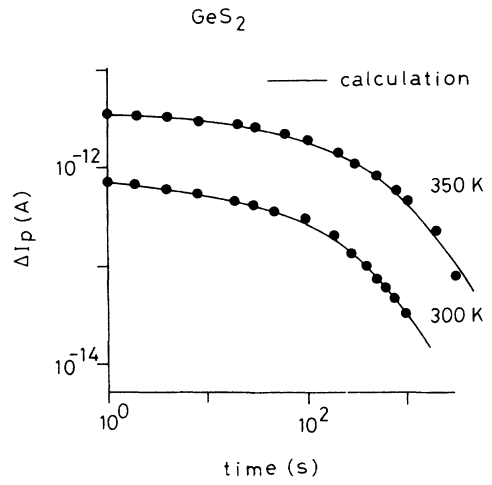


FIG. 5. Time-dependent change in photocurrent, $\Delta I_p$ for $a$-$GeS_2$ at 300 and 350 K. The solid lines are fits to Eq. (4).

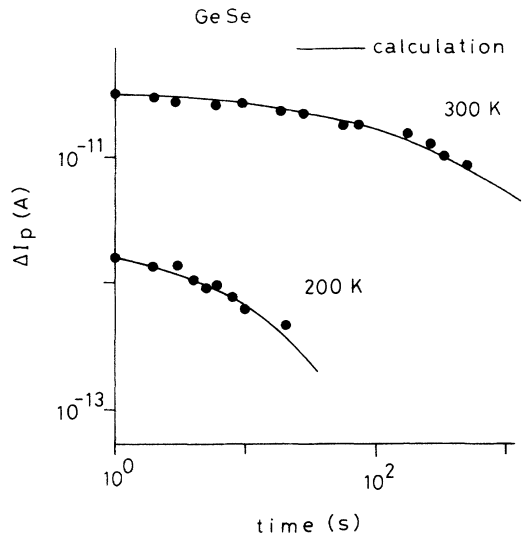


FIG. 7. Time-dependent change in photocurrent, $\Delta I_p$ for $a$-GeSe at 200 and 300 K. The solid lines are fits to Eq. (4).

culated results discussed in Sec. III.

A similar behavior of $I_p$ was also found for amorphous $As_2Se_3$, $GeS_2$, and $GeSe_2$ films. These are shown in Figs. 4–7. The Ge-rich material GeSe shows a slightly different behavior. The amount of the decrease in $I_p$ for room-temperature illumination is very much less than for the other materials studied, and is similar to that observed for $a$-Se. A decrease of $I_p$ at 300 K was not observed in $a$-Se.[7] This point will be discussed in a later section.

## III. A MODEL FOR THE DECREASE IN PHOTOCONDUCTIVITY

In previous papers,[7,8] we have suggested that the creation of widely separated random pairs of positively and negatively charged defect centers is responsible for the decrease in the photoconductivity. Such RP's result from bond-switching reactions at optically induced intimate pairs (conjugate pairs of charged defects, e.g., $P_4^+, C_1^-$, where $P$ and $C$ refer to pnictogen and chalcogen centers, and the superscript and subscript refer to the charge state and coordination number, respectively). Recent work on reversible photoinduced changes in the ac conductivity for $a$-$As_2S_3$ supports the notion of the formation of IP centers.[5,6] Part of the LESR signal can also originate from such IP centers.[1,2,11]

IP states would not act as efficient recombination centers for photocarriers, since they could be located far from a demarcation level that separates trapping and recombination levels and, as such, would not be expected to affect the photoconductivity (see the Appendix). The formation of IP ($Y$) and RP ($Z$) states is illustrated schematically in Figs. 8 and 9 for the case of stoichiometric $As_2S(Se)_3$ and $GeS(Se)_2$, respectively. The

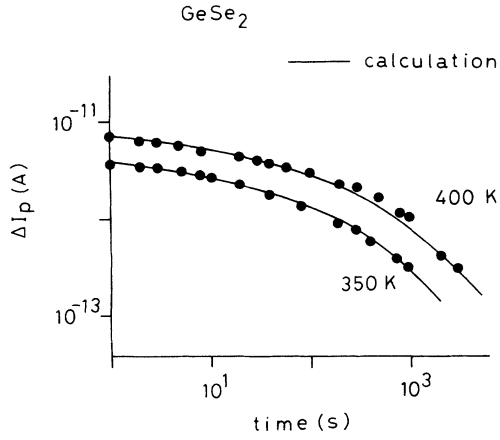


FIG. 6. Time-dependent change in photocurrent, $\Delta I_p$ for $a$-$GeSe_2$ at 350 and 400 K. The solid lines are fits to Eq. (4).

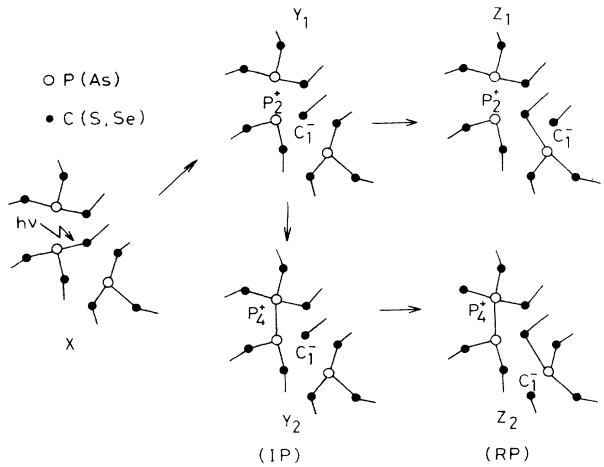


FIG. 8. Schematic illustration of the optical generation of intimate pairs (IP) of charged-defect states ($Y_1$, $Y_2$) from the chemically ordered ground-state structure of $a$-$As_2S(Se)_3$. Subsequent bond-switching reactions can lead to a large separation between the charged defects, i.e., random pairs [RP ($Z_1$,$Z_2$)].

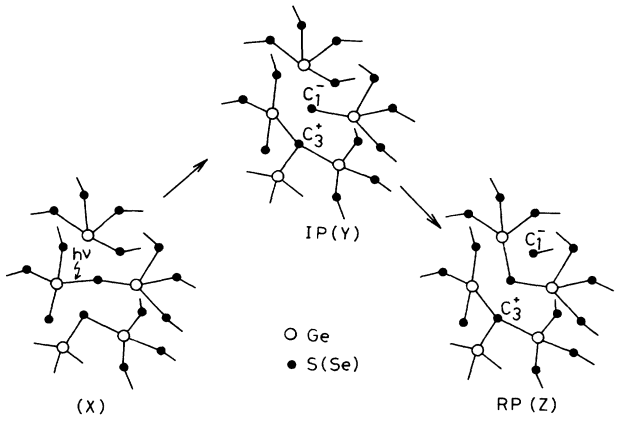


FIG. 9. Schematic illustration of the optical generation of the intimate-pair (IP) state ($Y$) from the chemically ordered ground-state structure of $a$-GeS $(Se)_2$. Random pairs [RP ($Z$)] are produced by subsequent bond-switching reactions of IP centers.

corresponding potential energies relating to the ground-state ($X$), IP ($Y$), and RP ($Z$) configurations are shown schematically in Fig. 10. RP's are formed by a DCBS process from IP's. Such a bond switching may be assisted by the energy released from electron-hole recombination (nonradiative multiphonon process). The IP center is produced from a free-exciton state by illumination,[1,12] not by the thermal energy $U_x$ shown in Fig. 10. IP centers do not seem to be stable above room temperature,[1,2,6] implying a small value for the energy $V_Y$ ($\lesssim kT_g$). On the other hand, since the RP state is stable near room temperature (but not stable at $T_g$),[7,8] $V_Z$ may be greater than $V_Y$ ($V_Z > kT_g$). It is thus expected that $V_Z > U_Y > V_Y$. In our earlier treatment,[7] it was assumed that $V_Z \gg kT_g$. Note here that the RP configuration is formed only via the intermediate IP state (as expected in Figs. 8 and 9; direct formation of RP seems to be difficult).

The rate equation for inducing RP centers via IP states can be written as

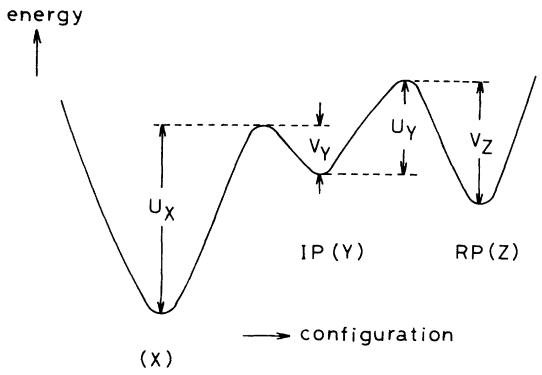


FIG. 10. Configurational-coordinate potential-energy diagram illustrating schematically the relative energies of the ground-state ($X$), IP ($Y$), and RP ($Z$) configurations.

$$dN_{\mathrm{RP}}/dt = k_p(\Gamma N_T - N_{\mathrm{RP}}) - k_r N_{\mathrm{RP}} , \quad (1)$$

where $N_{\mathrm{RP}}$ is the number of RP centers, $N_{\mathrm{RP}}=[D^+]=[D^-]$, $N_T$ is the total participating site density, $k_p$ is the promotion rate from IP, $k_r$ is the recovery rate from RP, and $\Gamma$ is a constant that should depend on the illumination intensity and, hence, $\Gamma N_T$ represents the number of IP centers. It is expected, however, that the factor $\Gamma$ is unity (independent of temperature and illumination intensity).[13] Assuming a time-dispersive reaction, the forward and backward reaction rates can be written as $k_p = At^{\alpha-1}$ and $k_r = Bt^{\alpha-1}$, respectively, where $A$ and $B$ are constants that should be related to nonradiative recombination rates at IP and RP centers, respectively (see the Appendix). By introducing recombination kinetics, we can treat light-enhanced bond switching (i.e., defect diffusion). The dispersion parameter $\alpha$ ($0<\alpha<1$) is assumed, for simplicity, to be the same for both the forward and backward reactions.[7,9,10]

$N_{\mathrm{RP}}$ is then given by

$$N_{\mathrm{RP}} = KN_T[1-\exp\{-(t/t_0)^\alpha\}] , \quad (2)$$

where $K = A/(A+B)$ and $t_0 = [\alpha/(A+B)]^{1/\alpha}$. The parameter $t_0$ is a measure of the RP creation time and which we denote here as the "effective creation time" of RP centers. It is expected that $t_0$ decreases with increasing illumination intensity and decreases with decreasing temperature if $\alpha$ is independent of temperature (see the Appendix). The photocurrent under conditions of thermal equilibrium can be expressed as

$$I_p = G/(N_0 + N_{\mathrm{RP}}) , \quad (3)$$

where $G$ is a constant and $N_0$ is the number of preexisting RP centers. In our previous treatment,[7] all free carriers (holes) were considered to be trapped by the induced RP centers and $N_0$ was not taken into account. At thermal equilibrium, however, this assumption may not be valid. Instead, Eq. (3) should be used to analyze the time dependence of $\Delta I_p$. The quantity $\Delta I_p (= I_p - I_\infty)$ is then given as

$$\Delta I_p(t) = \frac{G'}{(1+N_0/KN_T)\exp[(t/t_0)^\alpha]-1} . \quad (4)$$

Note again that we have introduced here $N_0$ (corresponding to the preexisting RP), which was not taken into consideration in our previous treatment.[7]

## IV. DISCUSSION

A decrease of the optical gap, viz. photodarkening (PD),[14] after illumination may also affect the magnitude of the photocurrent. An increase in the optical-absorption coefficient due to PD may increase the photocurrent; otherwise, the photocurrent will decrease with increasing surface recombination rate. However, as we used in our experiments nonmonochromatic light (halogen or mercury lamp), the photocurrent will not be affected so much by a small change of optical gap (PD). Thus, the effect of PD can be ignored here. Furthermore, the nonmonochromatic light used here would ensure bulk

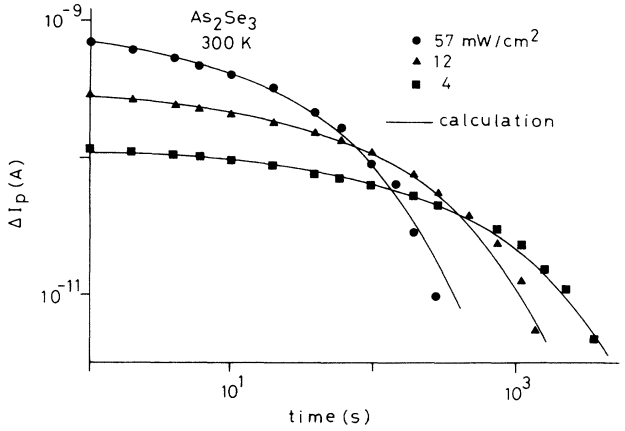


FIG. 11. Time-dependent change in photocurrent, $\Delta I_p$ for illumination intensities 57, 12, and 4 mW/cm$^2$ at 300 K in $a$-$As_2Se_3$.

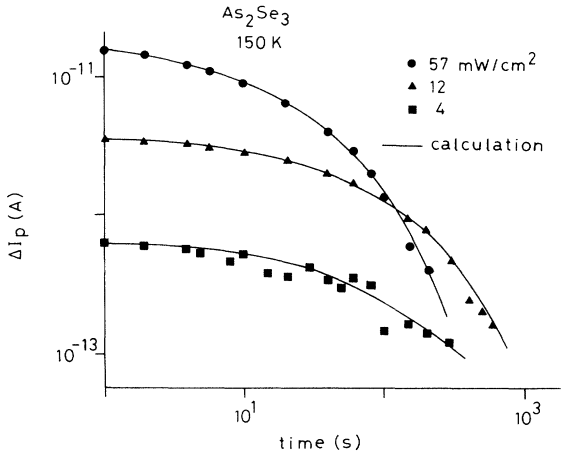


FIG. 12. Time-dependent change in photocurrent, $\Delta I_p$ for illumination intensities 57, 12, and 4 mW/cm$^2$ at 150 K in $a$-$As_2Se_3$.

excitation.

First, we should discuss the dependence of illumination intensity $L$ on $\Delta I_p(t)$ for different temperatures. Solid circles, triangles, and squares in Figs. 11 and 12 show the illumination-intensity-dependent $\Delta I_p(t)$ for temperatures 300 and 150 K in $As_2Se_3$, respectively. Neutral-density filters were used for these measurements.

The solid lines in Figs. 11 and 12 represent fits to Eq. (4). Fitting to the experimental data for each intensity produces values for parameters $\alpha$, $t_0$, and $N_0/KN_T$ and these are tabulated in Table II. As we expected in the preceding section, $t_0$ decreases with increasing illumination intensity. This is a manifestation of light-enhanced defect diffusion, which is very similar to the light-enhanced hydrogen diffusion (resulting in dangling-bond diffusion) observed in hydrogenated amorphous silicon ($a$-Si:H) films.[15] The parameter $N_0/KN_T$ depends on temperature and is independent of illumination intensity. These points will be discussed below.

The solid lines in Figs. 1–7 represent fits to Eq. (4). Fitting Eq. (4) to the experimental data (solid circles) produces values for parameters $\alpha$, $t_0$, and $N_0/KN_T$ and these are tabulated in Table III. Note that the $As_2Se_3$ sample here is not the same film (a different evaporation run) for which the intensity dependence was measured (Figs. 11 and 12) and the deduced parameters were not exactly reproducible. Parameter $\alpha$ is independent of temperature, although $\alpha$ for $As_2S_3$ and $As_2Se_3$ was treated as a temperature-dependent parameter in a previous paper.[8] The dashed line in Fig. 4 shows the curve for $\alpha=1$ (exponential), where $t_0=1.6\times10^3$ s and the same $\gamma=0.2$ were used, to compare with the stretched exponential function, indicating that experimental data could not fit to the simple exponential curve. It has also been reported for hydrogenated amorphous silicon ($a$-Si:H) that the creation of metastable defects obeys a stretched-exponential law.[16] The exponent $\alpha$ for $a$-Si:H, in contrast to amorphous chalcogenides, decreases with decreasing temperature. A detailed discussion of this is very difficult at present, since the origin of the dispersion parameter $\alpha$ is still not clear.[9,10]

The effective creation time $t_0$ decreases with decreasing temperature as tabulated in Table III. The electron-hole recombination probability at $D^-$ sites could decrease with increasing temperature, since the probability of thermal freeing of trapped holes at $D^-$ centers, and hence the factors $A$ and $B$, decrease with increasing temperature (see the Appendix).

Figures 13 and 14 show the detailed temperature dependence of $t_0$ and $N_0/KN_T$, respectively. These are shown by the solid squares and circles for $As_2S_3$ and $As_2Se_3$, respectively. A strong temperature dependence of $t_0$, which seems to have an activation energy, is ob-

TABLE II. Fitting parameters estimated from photocurrent measurements in $a$-$As_2Se_3$ as functions of illumination intensity and temperature. Dispersion parameter $\alpha$, effective creation time $t_0$, and $N_0/KN_T$.

| Temperature (K) | Illumination intensity $L$ (mW/cm$^2$) | Dispersion parameter $\alpha$ | Effective creation time $t_0$ (s) | $N_0/KN_T$ |
|---|---|---|---|---|
| 300 | 4 | 0.65 | 1180 | 0.6 |
| 300 | 12 | 0.65 | 285 | 0.6 |
| 300 | 57 | 0.65 | 58 | 0.6 |
| 150 | 4 | 0.65 | 200 | 1.0 |
| 150 | 12 | 0.65 | 150 | 1.0 |
| 150 | 57 | 0.65 | 35 | 1.0 |

TABLE III. Fitting parameters estimated from photocurrent measurements as a function of temperature. Dispersion parameter $\alpha$, effective creation time $t_0$, $I_\infty/I_p$ $(t=1)$, and $N_0/KN_T$.

| Chalcogenide | Dispersion parameter $\alpha$ | Effective creation time $t_0$ (s) | $I_\infty/I_p$ $(t=1)$ | $N_0/KN_T$ |
|---|---|---|---|---|
| $As_2S_3$ | 0.65 (350 K) | 24 (350 K) | 0.39 (350 K) | 0.1 (350 K) |
| | 0.65 (200 K) | 3 (200 K) | 0.59 (200 K) | 5.0 (200 K) |
| $As_3S_7$ | 0.75 (300 K) | 3.8 (300 K) | 0.29 (300 K) | 0.2 (300 K) |
| | 0.75 (200 K) | 3.3 (200 K) | 0.52 (200 K) | 10 (200 K) |
| AsS | 0.60 (300 K) | 45 (300 K) | 0.03 (300 K) | 0.2 (300 K) |
| | 0.60 (200 K) | 10 (200 K) | 0.41 (200 K) | 5.0 (200 K) |
| $As_2Se_3$ | 0.50 (350 K) | 900 (350 K) | 0.35 (350 K) | 0.2 (350 K) |
| | 0.50 (100 K) | 22 (100 K) | 0.37 (100 K) | 0.6 (100 K) |
| $GeS_2$ | 0.50 (350 K) | 278 (350 K) | 0.20 (350 K) | 1.5 (350 K) |
| | 0.50 (300 K) | 156 (300 K) | 0.73 (300 K) | 1.5 (300 K) |
| $GeSe_2$ | 0.45 (400 K) | 36 (400 K) | 0.51 (400 K) | 0.7 (400 K) |
| | 0.45 (350 K) | 167 (350 K) | 0.37 (350 K) | 1.0 (350 K) |
| GeSe | 0.40 (300 K) | 39 (300 K) | 0.89 (300 K) | 3.0 (300 K) |
| | 0.60 (200 K) | 10 (200 K) | 0.92 (200 K) | 2.0 (200 K) |

served at higher temperatures for both films. This may be related to the prediction that parameters $A$ and $B$ will have a temperature-activated term (see the Appendix). The temperature dependence of $N_0/KN_T$ for $As_2S_3$ is stronger than for $As_2Se_3$. The quantity $K^{-1}$, given by $1+B/A$, is a temperature-dependent parameter. The ratio $B/A$ can be proportional to

$$\exp[(W_{RP}-W_{IP})/kT]$$

with $W_{RP} > W_{IP}$, where $W_{RP}$ and $W_{IP}$ are the thermal energies for freeing trapped holes to the valence band (see also the Appendix and Fig. 15). Thus $K^{-1}$ should increase with decreasing temperature. Hence the parameter $N_0/KN_T$ increases with decreasing temperature, as observed experimentally in most cases (Tables II and III).

Since the ratio $B/A$ is independent of illumination intensity, the parameter $N_0/KN_T$ should also be independent of illumination intensity.

A decrease in $I_p$ for $a$-Se is not observed at 300 K, although a pronounced effect is observed if measured at 90 K.[7] Since the glass-transition temperature for this material is comparable to room temperature, the constant K is expected to be very small ($k_p \ll k_r$); as a consequence, the induced $N_{RP}$ should be very much smaller than $N_0$. No effect is therefore expected at higher temperatures. As shown in Fig. 7, a behavior similar to that exhibited

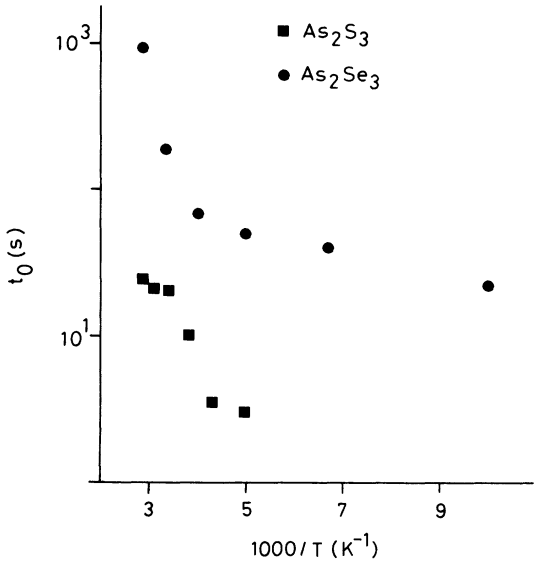


FIG. 13. The temperature dependence of $t_0$. Solid squares are for $a$-$As_2S_3$ and solid circles for $a$-$As_2Se_3$.

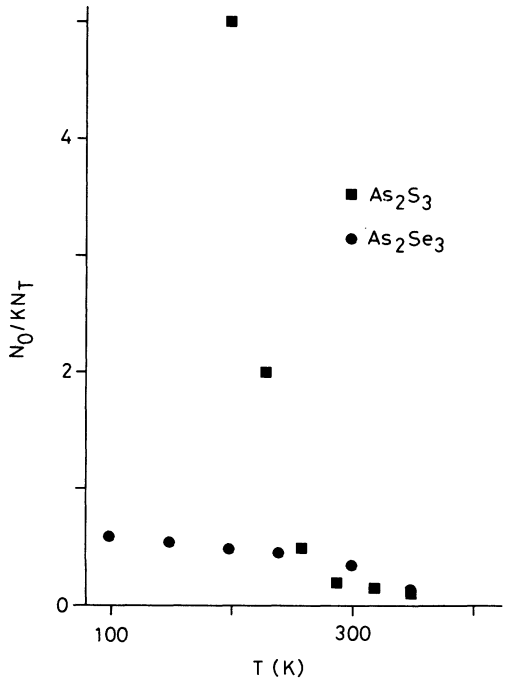


FIG. 14. The temperature dependence of the parameter $N_0/KN_T$. Solid squares are for $a$-$As_2S_3$ and solid circles for $As_2Se_3$.

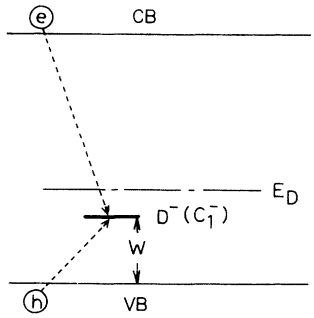


FIG. 15. Energy level for the $D^-$ ($C_1^-$) defect. $E_D$ is the demarcation energy level and $W$ is the thermal freeing energy of the trapped hole to the valence band. Free holes are first trapped into $D^-$ sites and then recombine with free electrons. The bond-switching reactions shown in Figs. 7 and 8 can be assisted by nonradiative recombination.

by $a$-Se is observed for $a$-GeSe. However, no pronounced decrease in $I_p$ is observed even at 200 K. As $T_g$ for $a$-GeSe is expected to be much higher than for $a$-Se,[17] since the introduction of Ge into Se increases $T_g$ for the glassy Ge-Se system,[18] the lack of a pronounced effect cannot be attributed to a low $T_g$ (large $k_r$), as discussed for $a$-Se. A large proportion of Ge-Ge bonds must exist in this material, which may result in a high density of thermal equilibrium (preexisting) defects, $N_0$. In fact, $I_p$ is very small for this material and is almost the same as the dark current at room temperature. Furthermore, due to the large proportion of Ge atoms, IP and RP centers may not be easy to produce as compared with Se (S)-rich Ge-Ge (S) systems (see Fig. 9). We thus expect $N_0 > N_{RP}$, resulting in a smaller decrease of $I_p$ for GeSe.

In the As-S system (see Figs. 1–3 and Table III), the effective creation time $t_0$ for $As_3S_7$ around room temperature is much shorter than for other materials. The recombination rate, which assists bond switching, for this material should be the greatest, which may be due to a larger $W$ (see the Appendix and Fig. 15). A larger $W$ should be attributed to a larger distortion energy related to the flexibility of its structural nature.[19] This can be attributed to a larger "atomic volume," which facilitates atomic relaxation processes such as bond switching. In fact, the atomic volume for $As_3S_7$ is larger than for $As_2S_3$ and $As_5S_5$.[20]

## V. CONCLUSION

Nonexponential photoconductivity decay during illumination, observed experimentally for a number of amorphous chalcogenide films (stoichiometric $As_2S_3$, $As_2Se_3$, $GeS_2$, and $GeSe_2$, and nonstoichiometric $As_3S_7$, AsS, and GeSe) can be described by stretched-exponential kinetics. The decrease in photoconductivity during illumination can be ascribed to the photoinduced creation of deep trapping states (well-separated charged defects). The initiation of defect creation is assumed to be the formation of a "self-trapped exciton" in the form of an intimate valence alternation pair. Following this, defect-conserved bond switching, which is enhanced by illumination, leading to defect migration and separation, results in the formation of metastable well-separated charged defects. The defect-creation kinetics are dominated by a time-dispersive reaction. By comparing a model calculation with the experimental data, we can estimate the physical parameters controlling the defect formation. There are many common features of the photodegradation between amorphous chalcogenides and hydrogenated amorphous silicon. These will be discussed in a future publication.

## ACKNOWLEDGMENTS

We would like to thank K. Hirose and T. Totani for help with the experiment. The XPS measurements were done at the Center of Instrumentation, Gifu University. We wish to thank The British Council (Tokyo) and Research Foundation for the Electrotechnology of Chubu for financial support.

## APPENDIX

The energy released by nonradiative recombination at charged dangling bonds in amorphous chalcogenides is expected to be approximately half the band gap.[19] This energy is sufficient to surmount the potential barrier $U_Y$ and $V_Z$ show in Fig. 10 and may assist bond switching. An example of such recombination at $D^-$ sites is shown in Fig. 15. Whether a center is to be considered as a trapping center or as a recombination center depends on the relative magnitude of the probability of thermal freeing of the trapped hole and the probability of recombination.[21,22] The ratio of recombination to trapping (i.e., "recombination yield," $f_r$) can then be defined as

$$f_r = \frac{r_p}{r_p + p_t \nu \exp(-W/kT)} \tag{A1}$$

and

$$r_p = n v S_n p_t \ , \tag{A2}$$

where $r_p$ is the recombination rate, and $p_t \nu \exp(-W/kT)$ is the rate of thermal freeing of the trapped holes. Here, $n$ is the density of free electrons in the conduction band, $v$ is their thermal velocity, $S_n$ is the capture cross section for electrons, $p_t$ is the density of $D^-$ occupied by (trapped) holes located at an energy $W$ above the valence band, and $\nu$ is the attempt-to-escape frequency. If the hole demarcation level[21,22] (corresponding to an equal probability of recombining with a free electron and of being thermally ejected to the valence band) lies well above the level of $D^-$, the probability of recombination can be much less than the probability of thermal freeing of trapped holes. Then $f_r$ can be written approximately as

$$f_r = n v S_n \nu^{-1} \exp(W/kT) \ . \tag{A3}$$

The above equation predicts that $f_r$ increases with increasing $n$ (proportional to light intensity) and increases

with decreasing temperature. It is expected that $W$ for IP ($W_{IP}$) is smaller than for RP ($W_{RP}$).[23] Then $f_r$ at a RP site $f_r$ (RP) is expected to be higher than at an IP site $f_r$ (IP). The constants $A$ and $B$ introduced in Sec. III should be proportional to $f_r(IP)$ and $f_r$ (RP), respectively, where the potential barriers $U_Y$ and $V_Z$ are ignored, since the energy released from nonradiative recombination ($\simeq 1$ eV) can be much larger than $U_Y$ and $V_Z$.


[1]D. K. Biegelsen and R. A. Street, Phys. Rev. Lett. **44**, 803 (1980).

[2]J. Hautala, W. D. Ohlsen, and P. C. Taylor, Phys. Rev. B **38**, 11 048 (1988).

[3]M. Abkowitz and R. C. Enck, Phys. Rev. B **27**, 7402 (1983).

[4]M. Abkowitz, G. M. T. Foley, J. M. Markovics, and A. C. Palumbo, in *Optical Effects in Amorphous Semiconductors,* Proceedings of the International Topical Conference on Optical Effects in Amorphous Semiconductors, edited by P. C. Taylor and S. G. Bishop, AIP Conf. Proc. No. 120 (AIP, New York, 1984), p. 117.

[5]K. Shimakawa, K. Hattori, and S. R. Elliott, Phys. Rev. B **36**, 7741 (1987).

[6]K. Shimakawa and S. R. Elliott, Phys. Rev. B **38**, 12 479 (1988).

[7]K. Shimakawa, S. Inami, and S. R. Elliott, Phys. Rev. B **42**, 11 857 (1990).

[8]K. Shimakawa, S. Inami, and S. R. Elliott, J. Non-Cryst. Solids **137&138**, 1017 (1991).

[9]H. Scher and E. W. Montroll, Phys. Rev. B **12**, 2455 (1975).

[10]M. F. Shlesinger, Ann. Rev. Phys. Chem. **39**, 269 (1988).

[11]S. R. Elliott and K. Shimakawa, Phys. Rev. B **42**, 9766 (1990).

[12]R. A. Street, Solid State Commun. **24**, 363 (1977).

[13]The rate equation for inducing IP centers can be given as $dN_{IP}/dt = c_p(N_T - N_{IP}) - c_r N_{IP}$, where $N_{IP}$ is the number of IP centers, $c_p$ is the inducing rate of IP centers, and $c_r$ is the recovery rate from IP to the ground state ($X$). The solution of this equation is $N_{IP} = \Gamma N_T[\exp(c_p + c_r)t - 1]$, where $\Gamma$ is $c_p/(c_p + c_r)$. It is expected that $c_p \gg c_r$ and hence $\Gamma \simeq 1$. The factor $c_p$ should also be much greater than $k_p$ (promotion rate from IP to RP) and the rate equation (1) can be valid under this condition.

[14]Ke. Tanaka, J. Non-Cryst. Solids **35&36**, 1023 (1980).

[15]P. V. Santos, N. M. Johnson, and R. A. Street, Phys. Rev. Lett. **67**, 2686 (1991).

[16]W. B. Jackson and D. M. Moyer, Phys. Rev. B **36**, 6217 (1987).

[17]$T_g$ for the $a$-GeSe film is unknown at present. The annealing temperature $T_a$ selected was tentatively 200 °C (see Table I). Using this $T_a$, reversible effects for $I_p$ and $E_o$ have been observed.

[18]Z. B. Borisova, *Glassy Semiconductors* (Plenum, New York, 1981), p. 104.

[19]N. F. Mott and E. A Davis, *Electronic Processes in Non-Crystalline Materials,* 2nd ed. (Clarendon, Oxford, 1979), p. 442.

[20]Ke. Tanaka, Phys. Rev. B **39**, 1270 (1989).

[21]A. Rose, *Concepts in Photoconductivity and Allied Problems,* (Interscience, Wiley, London, 1963), p. 11.

[22]R. H. Bube, *Photoconductivity of Solids* (Krieger, New York, 1960), p. 56.

[23]D. Adler, J. Phys. (Paris) Colloq. **42**, C4-3 (1981).